Active Site of Bee Venom Phospholipase A 2 : The Role of Histidine-34, Aspartate-64 and Tyrosine-87 †

ARTICLE *in* BIOCHEMISTRY · MAY 1996

Impact Factor: 3.02 · DOI: 10.1021/bi9528412 · Source: PubMed

6 AUTHORS, INCLUDING:

Robert R Annand
Stemgent, Lexington, United States
18 PUBLICATIONS **594** CITATIONS

SEE PROFILE

Maria Kontoyianni
Southern Illinois University Edwardsville
30 PUBLICATIONS **732** CITATIONS

SEE PROFILE

Active Site of Bee Venom Phospholipase A_2: The Role of Histidine-34, Aspartate-64 and Tyrosine-87[†]

Robert R. Annand,[‡] Maria Kontoyianni,[§,||] Julie E. Penzotti,[§] Thomas Dudler,[⊥] Terry P. Lybrand,[§] and Michael H. Gelb*[,‡]

Departments of Chemistry and Biochemistry and Center for Bioengineering, University of Washington, Seattle, Washington 98195, and SIAF, Davos, Switzerland.

Received November 30, 1995; Revised Manuscript Received February 9, 1996[⊗]

ABSTRACT: In bee venom phospholipase A_2, histidine-34 probably functions as a Brønsted base to deprotonate the attacking water. Aspartate-64 and tyrosine-87 form a hydrogen bonding network with histidine-34. We have prepared mutants at these positions and studied their kinetic properties. The mutant in which histidine-34 is changed to glutamine is catalytically inactive, while the mutants in which aspartate-64 is changed to asparagine or alanine (interfacial turnover numbers are reduced by 50−100-fold) or in which tyrosine-87 is changed to phenylalanine (no change in turnover number) retain good activity. The interfacial Michaelis constants are changed by less than 10-fold for all mutants. Molecular simulations suggest that mutation of aspartate-64 and tyrosine-87 should yield enzymes that retain a native-like structure and support catalysis. The pK_a of the histidine-34 imidazole was deduced from the pH-rate profile and from the pH dependence of the rate of histidine-34 alkylation by 2-bromo-4′-nitroacetophenone. The pK_a is increased about one-half unit by the tyrosine-87 mutation and reduced about one-half unit by the aspartate-64 to asparagine mutation, while in the aspartate-64 to alanine mutant the pK_a is unchanged. These pK_as are generally consistent with results of electrostatic calculations and suggest that the hydrogen bond between aspartate-64 and histidine-34 is not unusually strong. The hydrogen bonding network linking tyrosine-87 to aspartate-64 and aspartate-64 to histidine-34 is not critical for catalysis.

Phospholipase A_2 (PLA2)[1] catalyzes the hydrolysis of the *sn*-2 ester of glycerophospholipids. At least four groups of calcium-dependent PLA2s have been described, based on similarities of sequence and properties (Dennis, 1994). A number of small (14−18 kDa), disulfide-rich (5−7 disulfides per molecule) PLA2s have been isolated from a variety of sources, including reptile and insect venoms, pancreatic juices, platelets, and synovial fluid, and have been assigned to groups I, II, and III according to differences in amino acid sequence. Group IV PLA2 is an 85 kDa enzyme that has been purified from the cytosol of several different cell types (Glaser et al., 1993; Mayer & Marshall, 1993). In contrast to the small PLA2s, which require millimolar concentrations of Ca^{2+} for activity and show little phospholipid specificity (Gelb et al., 1995), the group IV PLA2 requires micromolar concentrations of Ca^{2+} for membrane binding and preferentially hydrolyzes phospholipids that contain arachidonic acid at the *sn*-2 position (Glaser et al., 1993; Mayer & Marshall, 1993). Recently, both group II and group IV PLA2s have been implicated in releasing free arachidonic acid from cell membranes for use in the biosynthesis of eicosanoids (Barbour & Dennis, 1993; Fonteh et al., 1994; Mounier et al., 1993; Roshak et al., 1994; Bartoli et al., 1994; Riendeau et al., 1994), suggesting a role for PLA2 in the inflammation process. In addition, receptors specific for low molecular weight PLA2s have been characterized on the surface of cells from several different tissues, including brain and muscle (Ishizaki et al., 1994; Lambeau et al., 1994). This suggests that other, as yet undefined, roles might exist for PLA2s in vivo.

Most of the venom and pancreatic PLA2s (groups I and II) are highly homologous (Dennis, 1994). The primary structure of the group III PLA2 from honeybee (*Apis mellifera*) venom (bvPLA2), in contrast, shows little homology to other small PLA2s, except in the region of the catalytic histidine and aspartic acid residues, the calcium binding loop, and certain cysteine residues (Kuchler et al., 1989). The remainder of the primary sequence of bvPLA2, as well as the gross tertiary structure, is distinct. For instance, bvPLA2 contains five intramolecular disulfide

[†] This research was supported by Grants HL36235 and GM562, a Research Career Development Award (to M.H.G.), predoctoral training grant fellowship GM08268 (to J.P.), and postdoctoral fellowship GM15464 (to R.R.A.), all from the National Institutes of Health, Grant MCB-9405405 (T.P.L.) from the National Science Foundation, and grants from Pittsburg Supercomputer Center and San Diego Supercomputer Center.

* To whom correspondence should be addressed.

[‡] Departments of Chemistry and Biochemistry, University of Washington.

[§] Center for Bioengineering, University of Washington.

[||] Current address: ZymoGenetics, 1201 Eastlake Ave. E., Seattle, WA 98102.

[⊥] SIAF; current address: Departments of Chemistry and Biochemistry, University of Washington, Seattle, WA 98195.

[⊗] Abstract published in *Advance ACS Abstracts,* March 15, 1996.

[1] Abbreviations: BSA, bovine serum albumin; bvPLA2, phospholipase A_2 from honeybee (*Apis mellifera)* venom; CD, circular dichroism; D-LPC, 3-hexadecyl-*sn*-glycero-1-phosphocholine; D64A, recombinant bvPLA2 with Asp-64 mutated to alanine; D64N, recombinant bvPLA2 with Asp-64 mutated to asparagine; DMPM, 1,2-dimyristoyl-*sn*-glycero-3-phosphomethanol; DPPC, 1,2-dipalmitoyl-*sn*-glycero-3-phosphocholine; H34Q, recombinant bvPLA2 with His-34 mutated to glutamine; HK-32, 1-*S*-octyl-2-heptylphosphonyl-*sn*-(1-thioglycero)-3-phosphoglycol; MES, 2-(*N*-morpholino)ethanesulfonic acid; PCR, polymerase chain reaction; PLA2, phospholipase A_2; PPyPM, 1-palmitoyl-2-(10-pyrenedecanoyl)-*sn*-glycero-3-phosphomethanol; SUV, small, unilamellar vesicle; THF, tetrahydrofuran; WT, wild type, recombinant bvPLA2; Y87F, recombinant bvPLA2 with Tyr-87 mutated to phenylalanine.

0006-2960/96/0435-4591$12.00/0

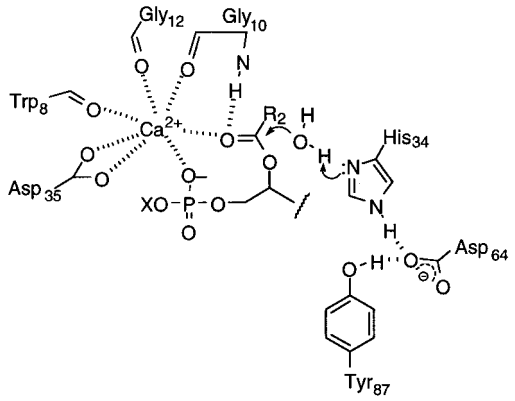

FIGURE 1: Structure of bvPLA2 active site and proposed catalytic mechanism.

bonds, while group I and II PLA2s contain seven disulfide bonds. Detailed examination of the tertiary structure of the active site of bvPLA2 reveals that the orientations of the catalytic water and the active site histidine and aspartate residues are very similar in bvPLA2 and porcine pancreatic PLA2, a representative member of the main group (Scott et al., 1990a). A model for the mechanism of hydrolysis of PLA2 has been proposed (Figure 1) which is reminiscent of that for the serine proteinase trypsin (Blow et al., 1969), except that a water molecule in bvPLA2 replaces the hydroxyl group of the catalytic Ser-195 in the trypsin as the nucleophile that attacks the carbonyl group at the reactive site on the substrate (Scott & Sigler, 1994b; Scott et al., 1990b; Verheij et al., 1980). The imidazole of His-34 functions as a Brønsted base to facilitate the deprotonation of the attacking nucleophilic water molecule. The carboxylate of Asp-64 is hydrogen bonded to the His-34 imidazole and presumably functions to stabilize the correct tautomer of the His-34 imidazole and to orient the imidazole productively, which facilitates deprotonation of the nucleophile or protonation of the leaving group. The carboxylate (Asp-64)−imidazole (His-34)−hydroxyl (water) triad in bvPLA2 is analogous to that found in chymotrypsin (Blow et al., 1969), where the Asp-102 and His-57 in chymotrypsin are analogous to Asp-64 and His-34 in bvPLA2 and the hydroxyl of Ser-195 in chymotrypsin is analogous to the catalytic water in bvPLA2. The essential calcium ion in bvPLA2 probably functions both to stabilize the oxyanion of the putative tetrahedral intermediate derived from the carbonyl oxygen of the substrate and to control the stereochemistry of productive substrate binding (Scott & Sigler, 1994a,b).

Phospholipase A_2 is the main allergen and immunogen in bee venom (King et al., 1976; Müller, 1990; Sobotka et al., 1976). Recent studies indicate that catalytic activity may be an important feature for the immunogenicity and allergenicity of bvPLA2 (Dudler et al., 1995). In vitro, unsensitized basophils give reduced degranulation when treated with the His-34 to glutamine mutant (H34Q) of bvPLA2, which is catalytically inactive, when compared to those treated with recombinant wild-type bvPLA2 (WT). In addition, H34Q is much less effective than WT in inducing IgG and IgE antibody responses when used to immunize mice. These results suggest that catalytic activity of the bvPLA2 plays a pivotal role in regulating the immune response of individuals exposed to this potent allergen.

In order to investigate the role of the active site residues in catalysis, we have studied mutants of bvPLA2 in which the active site aspartate residue has been changed to asparagine (D64N) or alanine (D64A), as well as a mutant in which a tyrosine residue which hydrogen bonds to the active site aspartate carboxylate is changed to phenylalanine (Y87F). In addition, a catalytically inactive mutant, in which the active site histidine residue is changed to glutamine (H34Q), was studied. Molecular simulation techniques were also used to explore the possible effects of the mutations on active site structures in catalytically viable mutants.

EXPERIMENTAL PROCEDURES

Materials. All reagents and buffers used were analytical grade obtained from standard suppliers. Oligonucleotides were synthesized on an Applied Biosystems (Foster City, CA) Model 380A DNA synthesizer and purified by butanol extraction (Sambrook et al., 1989). bvPLA2 expression plasmid p6xHis-Kall-BV-PLA2-#2 was previously described (Dudler et al., 1992). Restriction endonucleases and DNA modifying enzymes were purchased from New England Biolabs (Beverly, MA), Boehringer Mannheim Biochemicals (Indianapolis, IN), or Life Technologies/GibcoBRL (Gaithersburg, MD) and used according to the manufacturers' instructions. ULTROL grade guanidine hydrochloride was from Calbiochem (LaJolla, CA). Polymyxin B sulfate was from Sigma (St. Louis, MO). 2-Bromo-4′-nitroacetophenone was from Aldrich (Milwaukee, WI). D-LPC was a gift from M. K. Jain (University of Delaware). HK-32 was synthesized as described (Lin & Gelb, 1993). The plasmid for expression of H34Q was previously described (Dudler et al., 1995).

Construction of D64N, D64A, and Y87F. Oligonucleotide primers [TCA CAC GCG TCT TAG CTG CGA CTG CAA CGA CAA ATT C and the T7 primer (Stratagene, La Jolla, CA) for D64N, TTC CAC ACG CGT CTC AGC TGC GAC TGC GCA GAC AAA and TTG CGT ATA ATA TTT GCC CAT GGT GAA AAC for D64A or GGT AAA ATG TTT TTC AAC CTG ATC TAT and the T7 primer for Y87F] were used in a PCR-based method to introduce mutations into the bvPLA2 synthetic gene. PCR reactions (100 μL) contained 1 ng of template [the bvPLA2 synthetic gene in the pBluescript SK vector (Dudler et al., 1992) for D64N and Y87F, or p6xHis-Kall-BV-PLA2-#2 for D64A], 10 pmol of each primer, 0.2 mM each deoxyribonucleotide triphosphate, 0.1 mg/mL BSA, and 2 units of Vent DNA polymerase (New England Biolabs) in Vent polymerase buffer. The reaction was overlaid with 75 μL of mineral oil. Amplification was accomplished by repeating 1 min of denaturation at 96 °C, 1 min of annealing at 42 °C (D64A) or 50 °C (D64N, Y87F), and 2 min of extension at 72 °C for 35 cycles, followed by an additional 10 min extension. The PCR reaction mixtures were separated by agarose gel electrophoresis, and the amplified product was recovered using the Geneclean kit (Bio101, Inc., Vista, CA). For Y87F, a second PCR was performed using 0.5 μg of gel-purified product from the original PCR and 50 pmol of GGG GAT CCT CTC CGT TCC GC as primers. The remainder of the reaction components were as described above. The amplification conditions were the same as above, except that annealing temperature was 50 °C, and 20 cycles were performed. The purified PCR products were digested with the appropriate restriction enzymes (*Mlu*I and *Nco*I for D64A, *Mlu*I and

*Hin*dIII for D64N, and *Pst*I and *Hin*dIII for Y87F) and subcloned into the expression vector p6xHis-Kall-BV-PLA2-#2 using standard methods (Sambrook et al., 1989). The mutant plasmids were further purified using the QIAtip kit (QIAGEN) in order to verify the mutation by DNA sequencing using the DyeDeoxy sequencing kit on a Model 373A DNA Sequencer (Applied Biosystems, Foster City, CA).

Protein Purification. The bvPLA2 used in this study was produced in *Escherichia coli* as a fusion protein, in which a 15-residue peptide containing six histidine residues and a recognition site for the protease kallikrein is fused to the amino terminus of the mature protein (Dudler et al., 1992). The protein was isolated by immobilized metal affinity chromatography using Ni^{2+}-NTA-Agarose resin (QIAgen, Chatsworth, CA) under denaturing conditions, followed by in vitro refolding and SP-Sephadex chromatography, as described (Dudler et al., 1992). The fractions from the SP-Sephadex column containing bvPLA2 were pooled and dialyzed against 1 mM Tris, pH 8.0, concentrated using a Speed-Vac (Savant Instruments, Farmingdale, NY) to about 1 mg/mL, and stored at −20 °C. Alternatively, 0.02% NaN_3 was added directly to the pooled fractions, which were then stored at 4 °C. The bvPLA2s were used in this study without removing the fusion peptide.

Protein Concentration. The concentration of bvPLA2 was estimated either by UV spectroscopy ($E^{0.1\%}_{280nm} = 1.3$; Ghomashchi et al., 1991) or with the Bio-Rad protein assay kit (Bio-Rad, Richmond, CA) using, as a standard, a commercial bvPLA2 (Boehringer Mannheim Biochemicals, Indianapolis, IN) solution that had been standardized by UV.

Kinetic Parameters. The initial rate of hydrolysis in the scooting mode (v_0^*; see below) was determined using a titrimetric assay as described (Jain & Gelb, 1991). The assay contained 1 mM NaCl, 0.6 mM $CaCl_2$, 240 μM DMPM (as sonicated vesicles), 1 μM polymyxin B sulfate, and 0.02−0.25 μg/mL (1.3−16 nM) bvPLA2. Product formation was monitored by titration with 3 mM NaOH at 21 °C. The value of v_0^* was estimated from the initial slope of the progress curve.

The mole fraction of HK-32 (**1**) in DMPM vesicles

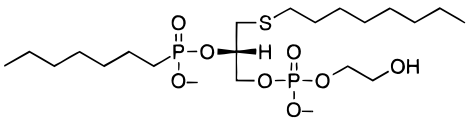

1: HK-32

required to reduce v_0^* 2-fold [$X_I(50)$] was determined as described (Lin & Gelb, 1993). Briefly, a few microliters of a stock solution of inhibitor in methanol was added to the pH-stat vessel, and v_0^* was measured as above. The data were fitted to eq 2 to determine $X_I(50)$.

The equilibrium dissociation constant (K_I^*) for the bvPLA2·HK-32 complex at the interface, in units of mole fraction inhibitor in the interface, was estimated from the rate of inactivation by 2-bromo-4′-nitroacetophenone in the presence or absence of inhibitor (Scrutton & Utter, 1965). The inactivation was carried out as for the pK_a determination (see below), except that the buffer was 50 mM sodium cacodylate, pH 7.3. The final reaction contained buffer, 0.6 mM $CaCl_2$, 100 mM NaCl, 2 mM D-LPC, 2 mM 2-bromo-4′-nitroacetophenone, 5% THF, 5% methanol, and 0−40 μM HK-32. The data were analyzed as described below to determine K_I^*.

pH-v_0^* Profile. The pH-v_0^* profiles of the bvPLA2s were obtained using a radiometric assay. The substrate was 1-palmitoyl-2-[9,10-$^3H_2$]palmitoyl-*sn*-glycero-3-phosphocholine (50 Ci/mmol; DuPont NEN, Boston, MA) present at 5.0 × 10^{-5} mole fraction in DMPM. Substrate vesicles were prepared by mixing a chloroform/methanol (2:1) solution of DMPM with the commercial solution of tritiated DPPC, evaporating the solvent under Ar, and then evacuating for 30 min. The lipid film was then hydrated in water to give a 4.6 mM lipid suspension, and SUVs were formed by freezing and sonicating the suspension (Jain & Gelb, 1991).

The reaction mixture (200 μL) contained buffer (20 mM each Tris, acetate, and MES, 0.6 mM $CaCl_2$, pH 4−10), 10 μL of SUV, and 0.25 μg/mL polymyxin B. The amount of enzyme (85−720 ng) and the time period over which the release of products is approximately linear were determined in a control experiment. After the appropriate time interval, a 100 μL aliquot of the reaction mix was quenched with 370 μL of 2:1:0.01 chloroform/methanol/concentrated HCl, 460 μL of 1:2:0.8 chloroform/methanol/water, 240 μL of chloroform, 240 μL of water, and 10 μL of 0.4 mg/mL myristic acid in dimethyl sulfoxide, and the released fatty acid was separated from phospholipid by silica gel chromatography, as described (Ghomashchi et al., 1992). The released [^{3}H]palmitate was quantitated by liquid scintillation using Bio-Safe scintillant (Research Products International, Mount Prospect, IL).

Estimation of the pK_a of His-34 by Alkylation. The pK_a of the active site histidine imidazole was estimated by measuring the rate of inactivation of bvPLA2 by 2-bromo-4′-nitroacetophenone at different pH values. Each 20 μL reaction contained Tris-acetate-MES buffer, 0.6 mM $CaCl_2$, 2 mM D-LPC, and bvPLA2 sufficient to give a good signal in the assay (5 μg/mL for WT). One microliter of a 40 mM THF solution of 2-bromo-4′-nitroacetophenone was added to initiate the reaction. At various time points (15 s to 4 h), 1 μL of the reaction was assayed for remaining PLA2 activity using the fluorescent substrate PPyPM as described (Dudler et al., 1992). Thin-layer chromatography on silica gel using 1:1 diethyl ether/petroleum ether showed little degradation of the alkylating agent during the course of the experiment if the pH was less than 8.0.

Guanidine Hydrochloride Denaturation. The stability of bvPLA2 toward denaturation by guanidine hydrochloride was measured using circular dichroism spectroscopy by the method used by Dupureur et al. (1992) for bovine pancreatic PLA2. Enzyme stock solutions were prepared by dialyzing the Tris-buffered enzyme stock against 1/10 × CD buffer (1 × CD buffer = 10 mM sodium borate, 0.1 mM EDTA, pH 8.0), diluting to 0.3 mg/mL with 1/10 × CD buffer, and concentrating 10-fold using a Speed-Vac. The bvPLA2 stock solution was diluted to 0.15 mg/mL in CD buffer containing various concentrations of guanidine hydrochloride, and the mixture was incubated at room temperature for 20 min. A background sample was prepared by mixing CD buffer with the same concentration of guanidine hydrochloride. The guanidine hydrochloride solutions were prepared by mixing CD buffer with a saturated (8.3 M) solution of ULTROL grade guanidine hydrochloride in CD buffer. A JA-720 (JASCO Instruments, Tokyo, Japan) spectropolarimeter was used to collect and signal average 10 scans per sample. After

subtracting a buffer background, the ellipticity at 222 nm was used to estimate the degree of denaturation, as described (Dupureur et al., 1992).

Data Analysis. Curve fitting was performed using either the Curve Fit program (Dr. Kevin Raner, CSIRO, Australia) or the curve fitting routines of the program Kalleidagraph (Abelbeck Software). Both programs gave the same results.

Structural Calculations. Structural models for all mutants examined in this study were generated using a combination of interactive molecular graphics model building, energy minimization, molecular dynamics, and (in the case of the D64N mutant) free energy perturbation calculations. The X-ray crystal structure for bvPLA2 was used as a starting model for all calculations (Scott et al., 1990a). The wild-type enzyme was first solvated in a water droplet extending ~30 Å from the center of the active site region, yielding a complex with 2260 water molecules. An enzyme−substrate complex was also modeled, based on the crystal structure of bvPLA2 with a transition state analog inhibitor (Scott et al., 1990a). In this complex, the phosphonate inhibitor was replaced with the homologous phosphatidylcholine lipid. This solvent complex contains 2250 water molecules, in addition to two crystallographic waters observed in the active site. For both free enzyme and enzyme−substrate complexes, all residues within ~12 Å of the active site center (defined operationally as the hydroxyl group of Tyr-87) were allowed to move freely during calculations. All other residues in the protein were kept fixed at X-ray crystallographic positions. All water molecules were allowed to move during the calculations as well. All water molecules were relaxed initially with several hundred steps of conjugate gradient energy minimization, followed by energy minimization of the entire system (excluding fixed residues outlined above) for 100−200 additional steps. Molecular dynamics simulations were then run for both the free enzyme and the enzyme−substrate complex. Each system was equilibrated for ~50 ps, followed by 50−75 ps of data collection. Isolated configurations were extracted from the bvPLA2 simulations and used as starting structures for generation of D64N, D64A, and Y87F mutant models. In the case of the Y87F mutant, it seems unlikely that the phenylalanine substitution will alter side chain packing interactions or active site structure significantly. Therefore, we generated Y87F model structures by simply deleting the *p*-hydroxyl group of Tyr-87, followed by 300−400 steps of energy minimization. For D64N and D64A mutant models, appropriate residue substitutions were made, followed by several hundred steps of energy minimization and then a molecular dynamics simulation protocol identical to that used for the wild-type enzyme. For the D64N mutant, a free energy perturbation technique (Straatsma & McCammon, 1992) was also used to generate model structures for comparison with the energy minimization/molecular dynamics protocol. In these calculations, Asp-64 was gradually converted to asparagine using the dynamically modified windows method (Pearlman & Kollman, 1989). All calculations (energy minimization, molecular dynamics, and free energy perturbation) were performed with standard all-atom potential functions (Weiner et al., 1986) using AMBER 4.0 (Pearlman et al., 1991). The SPC water model was used in all simulations (Berendsen et al., 1981). Partial charges for the phospholipid substrate were derived from molecular electrostatic potentials calculated with Gaussian 90 using a 6-31G* basis set and fitted to an atom-centered point charge model using the CHELPG program (Breneman & Wiberg, 1990). An integration time step of 1 fs was used in all molecular dynamics and free energy perturbation calculations, and all bond vibrations were constrained using the SHAKE algorithm (Ryckaert et al., 1977). A nonbonded interaction energy cutoff of 9 Å was employed for all calculations, and nonbonded interaction pair lists were updated every 25 steps.

pK_a Calculations. The effect of active site mutations D64N, D64A, and Y87F on the pKa of the catalytic His-34 residue was computed using Poisson−Boltzmann electrostatics calculations and a pK_a calculation protocol developed by Antosiewicz (Antosiewicz et al., 1994; Antosiewicz & Porschke, 1995). Briefly, this method entails (1) calculation of the self-ionization energy of each titratable group when free in aqueous solution, (2) calculation of the ionization energy of each titratable group in the neutral protein (i.e., all other titratable groups are held neutral, but partial charges from all atoms in the protein are included in the Poisson−Boltzmann calculations), (3) calculation of interaction energies for ionizable groups with each other, and (4) a Monte Carlo simulation to determine the lowest energy state(s) from among the 2^M possible ionization states in the protein, where M = number of titratable groups. Starting structures for the pK_a calculations were extracted from the molecular dynamics simulations outlined above, or the final structures from energy minimization in the case of the Y87F mutation. Four to six unique structures for each mutant were examined in the pK_a calculations, to ensure that results were not particularly dependent on conformation. The electrostatic potentials and electrostatic interaction energies needed to calculate ionization energies outlined in steps 1−3 were computed using a finite difference algorithm to solve the linearized Poisson−Boltzmann equation with the UHBD program (Davis et al., 1991). A coarse grid lattice (2.5 Å spacing) was used for initial estimates of electrostatic potentials (i.e., to compute long-range electrostatic contributions), followed by a focusing technique with successively higher resolution grids (1.20, 0.75, and 0.25 Å lattice point spacing) to facilitate convergence of short-range electrostatic interactions. All calculations were performed at T = 293 K, pH 7.0, and 150 mM ionic strength, with a solvent dielectric of 80.0, a protein dielectric of 20.0, and a 2.0 Å Stern layer. Previous tests have shown that a protein dielectric of 20.0 yields the best agreement with experimentally measured pK_a values (Antosiewicz et al., 1994). No explicit waters were included in the electrostatics calculations. Partial charges and van der Waals radii for the Poisson−Boltzmann calculations were taken from the latest AMBER potential functions (Cornell et al., 1995).

RESULTS

Characterization of Mutant bvPLA2s. Figure 1 shows the active site of bvPLA2 as determined by X-ray crystallography (Scott et al., 1990a). Side chains from the three residues Tyr-87, Asp-64, and His-34 form a hydrogen-bonding network with the catalytic water molecule, which adds to the *sn*-2 carbonyl of the substrate. To investigate the role of this network in catalysis, we separately mutated Tyr-87 to phenylalanine (Y87F), Asp-64 to asparagine (D64N) or to alanine (D64A), and His-34 to glutamine (H34Q). These active site mutants of bvPLA2 were created using a PCR-based strategy utilizing the abundant unique

Table 1: Catalytic Properties of Recombinant Bee Venom PLA2s[a]

PLA2	v_0^*[b] (s^{-1})	$X_I(50)$[c] (mol fraction)	K_I^*(mol fraction)	k_{cat}^* (s^{-1})	K_M^* (mol fraction)	k_{cat}^*/K_M^* (mol fraction^{-1} s^{-1})
WT	110	4.2×10^{-3}	7.1×10^{-4}	130	0.20	650
D64N	2.2	3.0×10^{-2}	1.1×10^{-3}	2.3	3.7×10^{-2}	62
D64A	1.2	2.4×10^{-2}	4.9×10^{-4}	1.2	1.9×10^{-2}	63
Y87F	55	3.8×10^{-4}	1.7×10^{-4}	100	0.81	123
H34Q	$<10^{-3}$	—[d]	—	—	—	

[a] Catalytic parameters were measured for the hydrolysis of DMPM in the scooting mode at pH 8 with inhibition by HK-32. [b] v_0^* for native bee venom PLA2 under the same conditions is 140 s^{-1}. [c] $X_I(50)$ of HK-32 for native bee venom PLA2 is 3.6×10^{-3}. [d] Not determined since this mutant has immeasurable activity.

restriction enzyme recognition sites in the synthetic bvPLA2 gene (Dudler et al., 1992). The entire coding region of all mutants were sequenced to verify that no additional mutations were present. The mutant bvPLA2s were isolated and refolded in vitro to obtain similar yields of recombinant protein (data not shown).

Kinetics of Interfacial Catalysis by bvPLA2s. Because the substrates of PLA2 are insoluble and form aggregates in aqueous suspension, the kinetic mechanism of catalysis by PLA2 is more complicated than that for enzymes that act on water-soluble substrates. In addition to the various rate constants that would be typical of an enzyme that acts on soluble substrates, the binding of PLA2 to the lipid aggregate must also be considered. By analyzing the hydrolysis of negatively charged lipid bilayer vesicles, Jain and co-workers showed that PLA2 remains tightly bound to the lipid vesicles throughout the course of the hydrolysis under low ionic strength conditions (Jain et al., 1986). This type of behavior is termed interfacial catalysis in the scooting mode. This method enables the progress curve for the hydrolysis to be described in terms of the integrated Michaelis−Menton equation (Berg et al., 1991). In SUVs of the anionic phospholipid DMPM, the mole fraction of substrate X_S drops quickly as bvPLA2 hydrolyzes the lipid. Therefore, v_0^*, the initial velocity per enzyme (i.e., $X_S \approx 1$), is best measured in the presence of polymyxin B, which promotes rapid intervesicle exchange of DMPM and maintains $X_S \approx 1$ for several minutes (Cajal et al., 1995; Jain et al., 1991a). Note, the asterisk is used to denote quantities that are measured for the action of PLA2 at the lipid−water interface. The velocity v_0^* is related to the interfacial Michaelis−Menton constants according to

$$v_0^* = k_{cat}^*/(1 + K_M^*) \quad (1)$$

where k_{cat}^* is the maximal velocity per enzyme for the hydrolysis of DMPM in the scooting mode, and K_M^* is the mole fraction of DMPM at which the velocity is $k_{cat}^*/2$ (Berg et al., 1991). Values of v_0^* for the various bvPLA2 mutants, measured with DMPM vesicles in the scooting mode in the presence of polymyxin B, are listed in Table 1. All of the recombinant PLA2s except H34Q show good catalytic activity; the v_0^* for H34Q is less than 1×10^{-5} that of native bvPLA2.

In order to determine k_{cat}^* and K_M^*, a different approach was necessary (Jain et al., 1991b). In the presence of a competitive inhibitor in DMPM SUVs at mole fraction X_I, it can be shown that

$$\frac{(v_0^*)^0}{(v_0^*)^I} = 1 + \left(\frac{1 + 1/K_I^*}{1 + 1/K_M^*}\right)\left(\frac{X_I}{1 - X_I}\right) \quad (2)$$

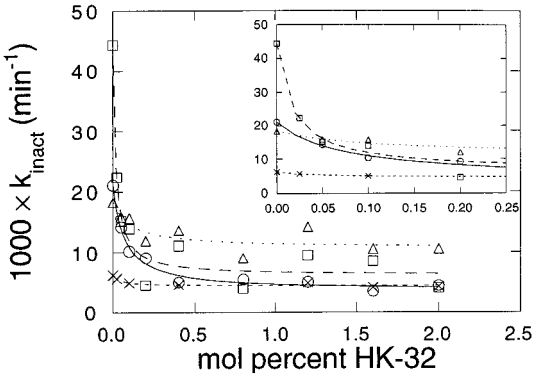

FIGURE 2: Protection of WT (circles), Y87F (squares), D64N (triangles), or D64A (crosses) by HK-32 against inactivation by 2-bromo-4′-nitroacetophenone in the presence of the neutral diluent D-LPC. Inset shows a close up of the low range of HK-32 mole fraction.

where $(v_0^*)^0$ and $(v_0^*)^I$ represent the initial rate per enzyme in the absence and presence of inhibitor, respectively (Berg et al., 1991). Equation 2 is the standard equation for a competitive inhibitor adapted for interfacial catalysis in the scooting mode. According to this equation, if K_I^* for an inhibitor can be determined by an independent method, K_M^* can be obtained from the reduction in velocity caused by the inhibitor at mole fraction X_I in the interface. In this work, the competitive inhibitor HK-32 (**1**) was used to estimate K_M^*; this phosphonate substrate analog is a good inhibitor of bvPLA2 (Lin & Gelb, 1993). To determine K_I^*, the rate of inactivation of bvPLA2 at the interface of the "neutral diluent" D-LPC by the alkylating agent 2-bromo-4′-nitroacetophenone, which modifies His-34, was measured in the presence of different mole fractions of the inhibitor HK-32 in the interface (Figure 2). [A neutral diluent is a compound that forms aggregates to which the PLA2 binds, but which does not enter the active site of the enzyme (Jain et al., 1991b).] Binding of the inhibitor to the active site of enzyme at the interface of a neutral diluent will protect the enzyme from inactivation. Previous studies have shown that D-LPC is a neutral diluent for bvPLA2 (Yu, Annand, Gelb, and Jain, manuscript in preparation). The dissociation constant K_I^* can be estimated from

$$k_{inact}^I/k_{inact}^0 = 1 - X_I(1 - k_I/k_0)/(K_I^* + X_I) \quad (3)$$

where k_{inact}^0 and k_{inact}^I are the pseudo-first-order rate constants for inactivation of enzyme in the absence or presence of inhibitor, and k_I and k_0 are the intrinsic rates of inactivation of the enzyme−inhibitor complex and free enzyme, respectively (Berg et al., 1991; Jain et al., 1991b; Scrutton & Utter, 1965). The values of K_I^* and $(1 - k_I/k_0)$ were estimated from a plot of k_{inact}^I/k_{inact}^0 vs X_I by fitting the data to eq 3.

Table 2: Stability of bvPLA2s toward Denaturation by Guanidine Hydrochloride

bvPLA2	$\Delta G^{H_2O}_{unfolding}$ (kcal mol^{-1})	m (kcal M^{-1} mol^{-1})
WT	2.26 ± 0.32	0.72 ± 0.10
H34Q	2.70 ± 0.36	1.29 ± 0.17
Y87F	1.63 ± 0.44	0.61 ± 0.16
D64N	2.00 ± 0.30	0.71 ± 0.10
D64A	1.97 ± 0.42	0.87 ± 0.14

The K_I^* values for the bvPLA2 mutants are summarized in Table 1.

Values of $X_I(50)$ and K_I^* were used to calculate K_M^* according to eq 2 with $(v_0^*)^0/(v_0^*)^I = 2$ and $X_I = X_I(50)$. Values of k_{cat}^* were calculated using the values of v_0^* and K_M^* according to eq 1. The results are listed in Table 1. These results show that the catalytic power (k_{cat}^*/K_M^*) is reduced 5-fold in the Y87F mutant and 10-fold in both the Asp-64 mutants relative to WT.

In addition to their catalytic activity, the stability of the mutant proteins toward guanidine hydrochloride denaturation was measured using CD spectroscopy. All of the recombinant proteins had virtually identical CD spectra in the absence of guanidine hydrochloride (data not shown). The denaturation curves were analyzed according to the model

$$\Delta G_{unfolding} = \Delta G^{H_2O}_{unfolding} + m[\text{guanidine hydrochloride}] \quad (4)$$

where m is proportional to the change in solvent-exposed surface area upon unfolding (Dill & Shortle, 1991), and the results are summarized in Table 2. All of the mutants have similar values for $\Delta G^{H_2O}_{unfolding}$ of about 2.0 to 2.5 kcal mol^{-1}. The value of m is about 0.7 kcal mol^{-1} M^{-1} for all of the PLA2s except H34Q, for which m is 1.3 kcal mol^{-1} M^{-1}. These results suggest that most of the mutations do not greatly affect the stability of the enzyme, but the H34Q mutation may cause a minor perturbation in the solvent-exposed surface of the protein.

pK$_a$ of His-34 Imidazole. We measured the pK_a of the active site imidazole of His-34 kinetically using two different techniques. First, the pH-v_0^* profile was measured for those recombinant PLA2s that had significant activity (Figure 3A,B). The data were fitted to the equation

$$v_0^* = (v_E + v_{EH+}[H^+]/K_a)/(1 + [H^+]/K_a) \quad (5)$$

where v_E and v_{EH+} are the rates for the unprotonated and protonated forms of the enzyme, respectively, and normalized such that $v_E = 100\%$. These curves show single inflection points with apparent pK_a values of 5.89 ± 0.12 for WT, 5.31 ± 0.08 for D64N, 6.40 ± 0.09 for Y87F, and 5.70 ± 0.07 for D64A. Thus, removal of the carboxylate of Asp-64 decreases the pK_a of the His-34 imidazole by about 0.5 when compared to WT or by about 1.1 when compared to Y87F.

To ascertain that the observed pH-rate differences actually reflect differences in protonation of His-34, we measured the pK_a of the His-34 imidazole directly by determining the effect of protonation of the imidazole on the rate of inactivation of the enzyme by the irreversible inhibitor 2-bromo-4′-nitroacetophenone (Figure 4A,B). The pseudo-first-order rate constant k_{inact} was measured at different pH

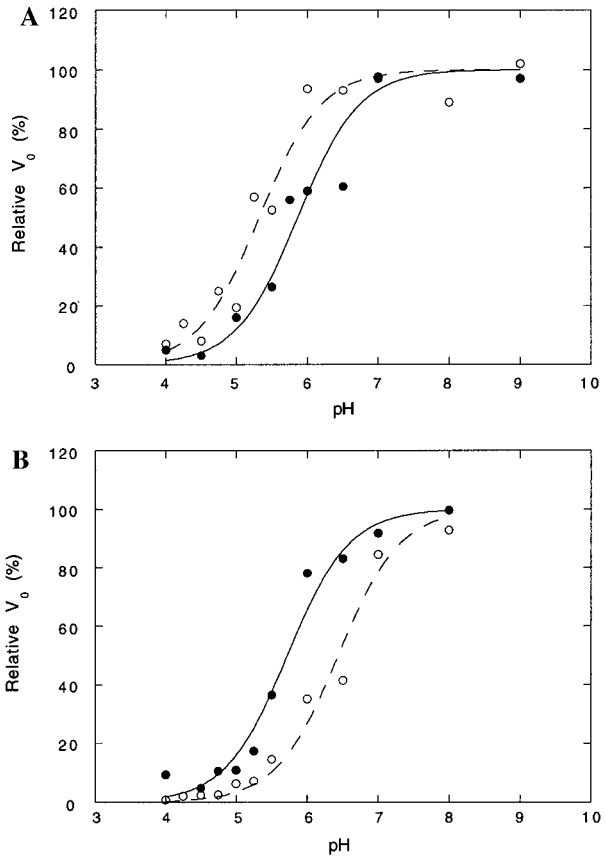

FIGURE 3: pH-v_0^* profiles of (A) WT (●, data; solid line, fit) and D64N (○, data; dashed line, fit) and (B) D64A (●, data; solid line, fit) and Y87F (○, data; dashed line, fit). The substrate was [^{3}H]-DPPC in DMPM. The lines represent a fit to eq 5. The data are plotted as percent of v_E.

values, and the data were fitted to the equation

$$k_{inact} = (k_E + k_{EH+}[H^+]/K_a)/(1 + [H^+]/K_a) \quad (6)$$

where k_E and k_{EH+} are the rate constants for inactivation of unprotonated and protonated enzyme, respectively. From these curves, apparent pK_as of 5.30 ± 0.33 for WT, 4.53 ± 0.47 for D64N, 5.75 ± 0.14 for Y87F, and 5.23 ± 0.40 for D64A were determined. These experiments were carried out with 2 mM 2-bromo-4′-nitroacetophenone, and, at pH 8.0; the half-time for alkylation increased 2-fold when 1 mM inactivator was used. This indicates that concentration of E*·2-bromo-4′-nitroacetophenone is less than then the concentration of E* (i.e., the equilibrium constant for dissociation of inactivator from E* is >2 mM) and that the alkylation reaction is first order in E* and in inactivator. Measuring the protonation state of the His-34 imidazole through the rate of its alkylation gave pK_a values that are about 0.6 units lower than those determined from the pH-v_0^* profile. This difference is probably due to the fact that the two experiments are measuring protonation of different species. The inactivation rate directly reflects the protonation state of the free enzyme, E*, as no substrate or other noncovalent active site ligand is present. The identity of the species whose protonation produces the pH-v_0^* profile is less obvious. Equation 1 shows that, in general, v_0^* depends on both k_{cat}^* and K_M^*. However, for these bvPLA2s, $K_M^* < 1$, so that $v_0^* \approx k_{cat}^*$. Therefore, the pH dependence of v_0^*, as does the pH dependence of k_{cat}^*, reflects the protonation of E*·S, rather than of free enzyme.

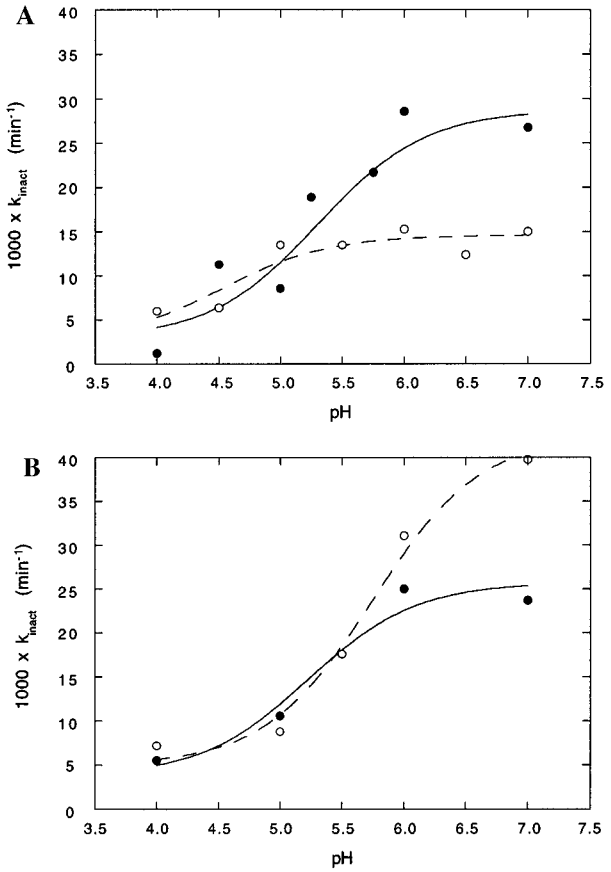

FIGURE 4: pH-k_{inact} profiles for the inactivation of (A) WT (●, data; solid line, fit) and D64N (○, data; dashed line, fit) and (B) D64A (●, data; solid line, fit) and Y87F (○, data; dashed line, fit) by 2-bromo-4′-nitroacetophenone. The pseudo-first-order rate constant k_{inact} was measured for the disappearance of activity over time when assayed at pH 9.0 using PPyPM as a substrate. The lines represent a fit to eq 6.

Structures of Single-Site Mutants. The results of all D64N structural calculations are completely consistent and independent of the computational protocol used (i.e., molecular dynamics simulation and free energy perturbation yield the same average structures). All of our perturbation trajectories (for both free enzyme and enzyme−substrate complexes) show that mutating Asp-64 to asparagine does not change the active site His-34 tautomer. Furthermore, the geometries of the active site residues His-34 and Tyr-87 are not significantly perturbed. The side chain conformation of His-34 in the D64N mutant and in the wild-type enzyme is in the preferred (trans, −) conformation (Table 3). Tyr-87 also has the same side chain conformation (t, 90) in the mutant and the WT structures. This is in agreement with analysis of the bovine pancreatic PLA2 D99N mutant crystal structure by Kumar et al. (1994). These structural predictions are also consistent with the enzyme activity measurements for the D64N mutant, which indicate that this mutation is accommodated in the active site.

In the WT enzyme both Tyr-87 and Nϵ2 of His-34 hydrogen bond to the aspartate residue (Figure 5A). In the course of our perturbation trajectories, the steric clash between the growing NH_2 group of D64N and the hydrogen atom of Nϵ2 of His-34 requires a reorientation of the Asn-64 side chain from the conformation assumed by the WT Asp-64. In four of five free enzyme perturbation trajectories, these steric problems are relieved by a rotation of Asn-64 which lifts it above the plane of the imidazole ring. In three of five enzyme−substrate complex trajectories, the Asn-64 side chain rotates to an orientation such that the carbonyl oxygen forms a hydrogen bond to Nϵ2 of His-34 and the amide NH_2 hydrogen bonds to the backbone carbonyl oxygen of Ser-60. Several other side chain rearrangements were also observed. Our simulations show that mutation of Asp-64 to Asn does not completely preserve the hydrogen bonding network linking the side chains of Tyr-87, His-34, and Asp-64 in the WT enzyme (Figure 5B). However, many of the specific hydrogen bonds present in the extended catalytic network, including those involving bound waters and other residues in the vicinity of the active site, are maintained. These extended interactions may restrict the rotation of the His-34 side chain. The restricted rotation of the His-34 side chain enables the formation of a good hydrogen bond between Nϵ2 of the imidazole ring and the carbonyl group of Asn-64. This hydrogen bond, in turn, ensures that the proper His-34 tautomer necessary for catalytic activity is maintained in the active site.

Table 3: Side Chain Conformations for His-34 and Tyr-87 in WT and D64N bvPLA2

enzyme trajectories	WT	D64N
His-34		
χ_1	−170.34 ± 8.62	−170.42 ± 6.62
χ_2	−129.86 ± 5.27	−120.36 ± 12.29
Tyr-87		
χ_1	−170.38 ± 4.49	−162.38 ± 6.55
χ_2	74.80 ± 6.77	88.70 ± 4.76
enzyme−substrate trajectories	**WT**	**D64N**
His-34		
χ_1	−173.48 ± 9.05	−176.14 ± 9.54
χ_2	−118.30 ± 11.10	−114.40 ± 10.56
Tyr-87		
χ_1	−174.12 ± 2.54	−162.38 ± 6.55
χ_2	85.90 ± 15.41	80.22 ± 10.63
residue 64	**E**	**E·S**
Asp-64		
χ_1	−158.40 ± 6.40	−84.26 ± 5.05
χ_2	−101.46 ± 7.40	151.94 ± 12.12
Asn-64		
χ_1	−172.98 ± 10.27	−105.90 ± 34.59
χ_2	−56.74 ± 69.88	−158.42 ± 54.19

The D64A mutant likewise exhibits relatively little structural alteration. The most noticeable, consistent change seen in simulations of this mutant is the loss of one of the two active-site water molecules observed in the reference crystal structure. This water escapes to the bulk environment in all D64A simulations, and no further exchange with other bulk solvent molecules is observed during the course of our simulations. All other hydrogen bonding contacts are generally maintained as seen in the wild-type structure.

The Y87F mutant models do not deviate in any noticeable way from the wild-type structure, except that several hydrogen bonds formed by the *p*-hydroxyl group of Tyr-87 to Asp-64 and to an active site water are lost. Since both of these residues form other hydrogen bonding contacts, the Y87F mutation does not appear to perturb the location or orientation of either Asp-64 or the water molecule in any significant way.

Computed pK_a Shifts for Single-Site Mutants. The calculated pK_a value for Asp-64 in wild-type bvPLA2 is 3.4 ±

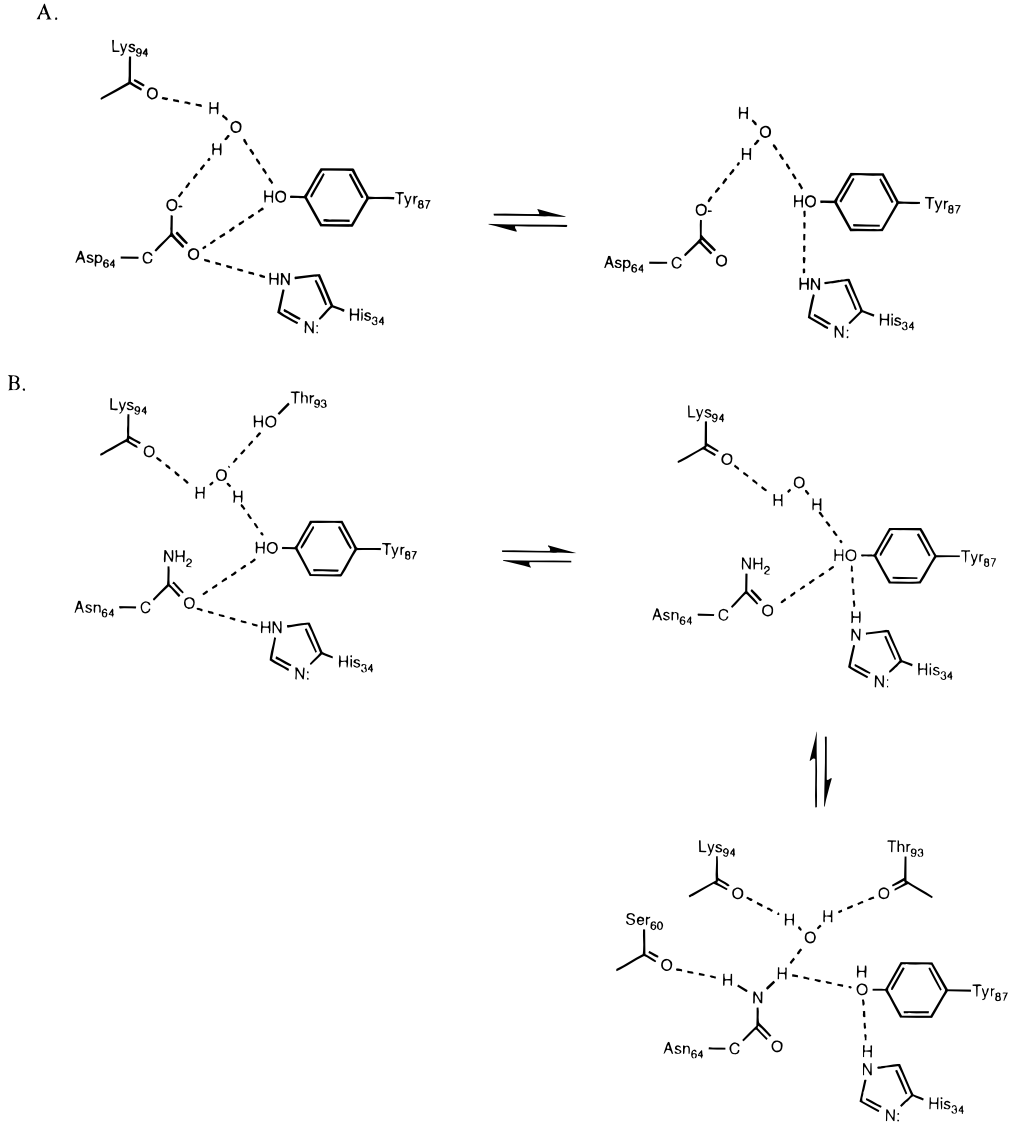

FIGURE 5: Hydrogen bonding scheme and fluctuations for (A) WT and (B) D64N bvPLA2 observed in molecular dynamics trajectories.

0.1, and computed pK_a values for His-34 are 5.5 ± 0.4 for WT, 4.1 ± 0.7 for D64N, 5.7 ± 0.2 for Y87F, and 4.0 ± 0.5 for D64A. As can be seen from these data, the computed results are in excellent agreement with the experimental measurements performed in the absence of substrate, except for the D64A mutation, where we predict a significant reduction in the pK_a of His-34 from 5.5 (WT) to 4.0 for the alanine mutant. In contrast, the experimental measurement suggests only a small downward shift for the His-34 pK_a in response to this mutation.

We also performed several pK_a calculations to probe the role of the active site calcium ion in these systems. In these calculations, we removed the calcium ion from the enzyme and ran the pK_a calculations again as described above. We consistently find that removal of the active site calcium ion results in an increase in the His-34 pK_a by ~1.5−2.0 units. This increase in pK_a is independent of other active site mutations, so that His-34 has a pK_a of ~7.0 in the wild-type enzyme and a pK_a of ~6.0 in the D64N mutant, for example. Unfortunately, due to the instability of 2-bromo-4′-nitroacetophenone at alkaline pH and the catalytic inactivity of bvPLA2 in the absence of calcium, these calculations could not be verified experimentally by the approaches used in this work.

DISCUSSION

The hydroxyl−imidazole−carboxylate triad is a common motif in the active sites of enzymes that hydrolyze esters and amides. Although the triad was first described in 1969 in chymotrypsin (Blow et al., 1969), the role of the carboxylate is still the subject of some controversy. In this paper, we have analyzed the effect of the carboxylate on the function of bvPLA$_2$. Replacement of Asp-64 with asparagine results in a modest reduction of catalytic efficiency (56-fold in k^*_{cat} and 10-fold in k^*_{cat}/K^*_M), and similar results were obtained with PLA2s from bovine pancreas [19-fold in k^*_{cat} and 7-fold in k^*_{cat}/K^*_M (Kumar et al., 1994)] and from porcine pancreas [25-fold in k^*_{cat} and 33-fold in k^*_{cat}/K^*_M (Kuipers et al., 1990)]. Although in some cases different assays were used to study these mutants, it is clear that for group I and III PLA2s the replacement of aspartate with asparagine produces a much smaller effect on the kinetic parameters than does the corresponding mutation in trypsin (20 000-fold in k_{cat} and 25 000-fold in k_{cat}/K_M (Craik et al., 1987)]. This large difference between PLA2s and trypsin is probably due to the differences in hydrogen-bonding environments of the aspartate. In trypsin, the carboxylate oxygen of aspartate-102 that is not hydrogen-bonded to

histidine accepts two hydrogen bonds from backbone amide NH groups. Thus, when aspartate is replaced by asparagine, the amide NH_2 group is forced to point toward the imidazole ring, which in turn requires that the imidazole adopt a tautomeric state that prevents it from acting as a Brønsted base in removing the proton from serine-195 (Sprang et al., 1987). With PLA2s, the carboxylate oxygen of aspartate that is not hydrogen bonded to imidazole engages in hydrogen bonds with the hydroxyl groups of tyrosine and water. Such hydrogen bond donors can also serve as acceptors such that the amide NH_2 of asparagine can occupy the same position as this carboxylate oxygen of aspartate. This leaves the carbonyl oxygen of asparagine in a position to accept a hydrogen bond from imidazole, thus leaving the imidiazole in the proper tautomer state for catalysis. This idea is supported by the high catalytic activities of the PLA2 mutants, by the X-ray structure of the bovine mutant (Kumar et al., 1994), and by the molecular simulations of the present study.

Based on the above arguments, the only difference between WT and D64N is the lack of a negative charge at position 64. This is expected to lower the pK_a of the imidazolium of His-34. Indeed, the kinetic and His-34 alkylation studies strongly suggest that the pK_a of this histidine is about 0.7 units lower in the mutant compared to WT, and this result is in agreement with the pK_a calculations. It has been recently proposed that Asp-102 and His-57 of serine proteases are engaged in an exceptionally strong (low barrier) hydrogen bond (Frey et al., 1994). Such hydrogen bonds are thought to form when the pK_a of the hydrogen bond donor and pK_a of the conjugate acid of the hydrogen acceptor are of similar value. It is clear from the present results that such a strong hydrogen bond does not form in bvPLA2. A strong hydrogen bond is not possible for D64N because the carbonyl oxygen of the asparagine side chain is a poor base. The fact that the pK_a of WT and D64N differ by only 0.7 units indicates that the hydrogen bond in the WT enzyme is not exceptionally strong (a change of 0.7 pK_a units corresponds to a change in free energy of only 1 kcal/mol). In addition, the calculations suggest that the shift in pK_a can be accounted for by electrostatics alone. It is possible that a low barrier hydrogen bond does not form in PLA2 because the pK_a values of Asp-64 and His-34 may be too dissimilar to enable formation of a strong hydrogen bond, as our electrostatics calculations predict pK_a values for Asp-64 of 3.4 $\pm$ 0.1 and His-34 of 5.5 $\pm$ 0.4 in wild-type bvPLA2.

Since bvPLA2 mutants lacking the Asp-64 carboxylate are clearly able to catalyze the hydrolysis of phospholipids, and thus Asp-64 is not essential for catalysis, why is the His-Asp catalytic diad a universal feature of PLA2? The carboxylate could serve to anchor the imidazole into the optimal conformation for catalysis. The good activity of the D64A mutant, whose imidazole should have considerably more conformational flexibility than that of WT or D64N, suggests that this conformational stabilization plays only a minor role. However, for D64A, we cannot exclude the possibility that a water molecule hydrogen bonded to His-34 replaces the carboxylate of Asp-64. The fact that His-34 in D64N is a weaker base than in WT requires that His-34 in D64N is a poorer Brønsted base and is thus less effective in removing the proton from the water that attacks the carbonyl group of the ester substrate. According to Bronsted theory, a 0.7 unit change in the pK_a of His-34 will lead to a maximum change in the rate constant for attack of water onto the substrate ester of $10^{0.7}$ (5-fold) (Jencks, 1969). However, the fact that k^*_{cat} of D64N is 56-fold lower than that for WT implies that Asp-64 is serving other roles in catalysis that are not obvious. [Although the pH-rate profile for D64N is shifted relative to WT, v_0^* for both enzymes was measured at pH 8, where the activity is maximum for both enzymes (Figure 3A).]

The pH behavior of several models for carboxylate−imidazole couple in enzyme active sites has been examined. Compounds containing a hydrogen bond involving an imidazole NH and the *anti* lone pair on the carboxylate generally have a pK_a about 0.6−0.9 units higher than similar analogs without the hydrogen bond. Examples include **2**

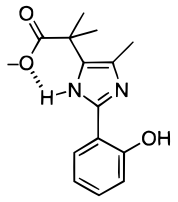

2

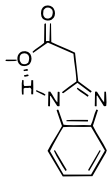

3

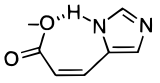

4

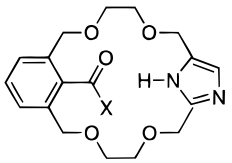

5: X = NH_2, O^-

(ΔpK_a = 0.76; Rogers & Bruice, 1974), **3** (ΔpK_a = 0.7; Komiyama & Bender, 1977), **4** (ΔpK_a = 0.9; Roberts et al., 1982), and N_α-acetylhistidine (ΔpK_a = 0.62; Tanokura, 1983). These effects are very similar to that seen in bvPLA2 which also utilizes the *anti* lone pair of Asp-64. Zimmerman and Cramer (1988) have synthesized model compounds **5**, in which an imidazole is hydrogen bonded to the *syn* lone pair of a carboxylate or to an amide, and measured a ΔpK_a of 1.35 for the imidazole by ^{1}H NMR. Craik et al. (1987) have analyzed wild-type and mutant trypsin by measuring pH-rate profiles. They find that the pK_a of the His-58 imidazole decreases by 1.5 units when Asp-102 is changed to Asn. The pK_a differences in trypsin and **5** are somewhat larger than the effect of the Asp-64 to Asn-64 change in bvPLA2, probably because trypsin and **5** contain hydrogen bonds to the more basic *syn* lone pair on the carboxylate, rather than to the *anti* lone pair, as found in bvPLA2.

It is remarkable that the pK_a values for His-34 in D64A and in WT are similar. How can the removal of a negative charge in the vicinity of His-34 lead to no change in its pK_a? The calculated and experimental values of pK_a are in excellent agreement except for D64A. This discrepancy may be due in part to the omission of explicit water molecules in the active site of the enzyme. It appears from our model building and structural simulations that in the case of D64A it may be possible for a water molecule to shift in the active site, potentially assuming the role of the wild-type Asp-64 as a hydrogen-bonding partner for His-34. Our continuum model electrostatics calculations cannot account for such a possible rearrangement, which could contribute to the

dramatic pK_a decrease we compute for His-34 in the D64A mutant. However, even if this were the case, D64A would still lack the negative charge present in WT. Apparently other factors contribute to the pK_a value of His-34 in D64A that are not obvious.

Replacement of Tyr-87 with phenylalanine produces a 1.3-fold reduction in k^*_{cat} and a 5-fold reduction in k^*_{cat}/K^*_M. The analogous residue in pancreatic PLA2s is Tyr-52, and replacement of this with phenylalanine leads to virtually no change in the kinetic parameters (Kuipers et al., 1990; Dupureur et al., 1992). Thus, these well-conserved tyrosines are not important for the catalytic efficiency of group I and III PLA2s. Replacement of tyrosine with phenylalanine produces only a modest effect on the stability of bvPLA2 and bovine pancreatic PLA2 (Dupureur et al., 1992) ($\Delta G^{H_2O}_{unfolding}$ is reduced by <2 kcal/mol for both enzymes).

The results presented in this work and in previous studies (Kuipers et al., 1990; Dupureur et al., 1990, 1992; Kumar et al., 1994) show that the active site hydrogen-bonding network involving the side chains of the active-site histidine, aspartate, and tyrosine residues of group I and III PLA2s is not essential for the catalytic process. Mutation of the active-site histidine of bvPLA2 and of bovine pancreatic PLA2 (Li & Tsai, 1993) to glutamine causes a complete loss of catalytic activity, consistent with its proposed role as the active site Brønsted base.

ACKNOWLEDGMENT

We thank Mahendra Jain for the gift of the D-LPC and Kelly J. Kirkpatrick for excellent technical assistance.

REFERENCES

Antosiewicz, J., & Porschke, D. (1995) *Biophys. J. 68*, 655.
Antosiewicz, J., McCammon, J. A., & Gilson, M. K. (1994) *J. Mol. Biol. 238*, 415.
Barbour, S. E., & Dennis, E. A. (1993) *J. Biol. Chem. 268*, 21875.
Bartoli, F., Lin, H.-K., Ghomashchi, F., Gelb, M. H., Jain, M. K., & Apitz-Castro, R. (1994) *J. Biol. Chem. 269*, 15625.
Berendsen, H. J. C., Postma, J. P. M., & van Gunsteren, W. F. (1981) in *Intermolecular Forces* (Pullman, B., Ed.) pp 331, Reidel, Dordrecht, The Netherlands.
Berg, O. G., Yu, B.-Z., Rogers, J., & Jain, M. K. (1991) *Biochemistry 30*, 7283.
Blow, D. M., Birktoft, J. J., & Hartley, B. S. (1969) *Nature 221*, 337.
Breneman, C. M., & Wiberg, K. B. (1990) *J. Comput. Chem. 11*, 361.
Cajal, Y., Berg, O. G., & Jain, M. K. (1995) *Biochem. Biophys. Res. Commun. 210*, 746.
Cornell, W. D., Cieplak, P., Bayly, C. I., Gould, I. R., Merz, K. M., Jr., Ferguson, D. M., Spellmeyer, D. C., Fox, T., Caldwell, J. C., & Kollman, P. A. (1995) *J. Am. Chem. Soc. 117*, 5179.
Craik, C. S., Roczniak, S., Largman, C., & Rutter, W. J. (1987) *Science 237*, 909.
Davis, M. E., Madura, J. D., Sines, J., Luty, B. A., Allison, S. A., & McCammon, J. A. (1991) *Methods Enzymol. 202*, 473.
Dennis, E. A. (1994) *J. Biol. Chem. 269*, 13057.
Dill, K. A., & Shortle, D. (1991) *Annu. Rev. Biochem. 60*, 795.
Dudler, T., Chen, W.-Q., Wang, S., Schneider, T., Annand, Dempcy, R. O., R. R., Crameri, R., Gmachl, M., Suter, M., & Gelb, M. H. (1992) *Biochim. Biophys. Acta 1165*, 201.
Dudler, T., Machado, D. C., Kolbe, L., Annand, R. R., Rhodes, N., Gelb, M. H., Koelsch, E., Suter, M., & Helm, B. A. (1995) *J. Immunol. 155*, 2605.
Dupureur, C. M., Deng, T., Kwak, J.-G., Noel, J. P., & Tsai, M.-D. (1990) *J. Am. Chem. Soc. 112*, 7094.
Dupureur, C. M., Yu, B.-Z., Jain, M. K., Noel, J. P., Deng, T., Li, Y., Byeon, I.-J., & Tsai, M.-D. (1992) *Biochemistry 31*, 6402.
Fonteh, A. N., Bass, D. A., Marshall, L. A., Seeds, M., Samet, J. M., & Chilton, F. H. (1994) *J. Immunol. 152*, 5438.
Frey, P. A., Whitt, S. A., & Tobin, J. B. (1994) *Science 264*, 1927.
Gelb, M. H., Jain, M. K., Hanel, A. M., & Berg, O. G. (1995) *Annu. Rev. Biochem. 64*, 653.
Ghomashchi, F., Yu, B. Z., Mihelich, E. D., Jain, M. K., & Gelb, M. H. (1991) *Biochemistry 30*, 9559.
Ghomashchi, F., Schüttel, S., Jain, M. K., & Gelb, M. H. (1992) *Biochemistry 31*, 3814.
Glaser, K. B., Mobilio, D., Chang, J. Y., & Senko, N. (1993) *Trends Pharmacol. Sci. 14*, 92.
Ishizaki, J., Hanasaki, K., Higashino, K.-i., Kishino, J., Kikuchi, N., Ohara, O., & Arita, H. (1994) *J. Biol. Chem. 269*, 5897.
Jain, M. K., & Gelb, M. H. (1991) *Methods Enzymol. 197*, 112.
Jain, M. K., Rogers, J., Jahagirdar, D. V., Marecek, J. F., & Ramirez, F. (1986) *Biochim. Biophys. Acta 860*, 435.
Jain, M. K., Rogers, J., Berg, O., & Gelb, M. H. (1991a) *Biochemistry 30*, 7340.
Jain, M. K., Yu, B.-Z., Rogers, J., Ranadive, G. N., & Berg, O. G. (1991b) *Biochemistry 30*, 7306.
Jencks, W. P. (1969) *Catalysis in Chemistry and Biology*, McGraw-Hill, New York.
King, T. P., Sobotka, A. K., Kochoumian, L., & Lichtenstein, L. M. (1976) *Arch. Biochem. Biophys. 172*, 661.
Komiyama, M., & Bender, M. L. (1977) *Bioorg. Chem. 6*, 13.
Kuchler, K., Gmachl, M., Sippl, M. J., & Kreil, G. (1989) *Eur. J. Biochem. 184*, 249.
Kuipers, O. P., Franken, P. A., Hendriks, R., Verheij, H. M., & De Haas, G. H. (1990) *Protein Eng. 4*, 199.
Kumar, A., Sekharudu, C., Ramakrishnan, B., Dupureur, C. M., Zhu, H., Tsai, M.-D., & Sundaralingam, M. (1994) *Protein Sci. 3*, 2082.
Lambeau, G., Ancian, P., Barhanin, F., & Lazdunski, M. (1994) *J. Biol. Chem. 269*, 1575.
Li, Y., & Tsai, M.-D. (1993) *J. Am. Chem. Soc. 115*, 8523.
Lin, H.-K., & Gelb, M. H. (1993) *J. Am. Chem. Soc. 115*, 3932.
Mayer, R. J., & Marshall, L. A. (1993) *FASEB J. 7*, 339.
Mounier, C., Faili, A., Vargaftig, B. B., Bon, C., & Hatmi, M. (1993) *Eur. J. Biochem. 216*, 169.
Müller, U. R. (1990) *Insect Sting Allergy, Clinical Picture, Diagnosis, and Treatment*, G. Fischer, Stuttgart.
Pearlman, D. A., & Kollman, P. A. (1989) *J. Chem. Phys. 90*, 2460.
Pearlman, D. A., Case, D. A., Caldwell, J. C., Seibel, G. L., Singh, U. C., Weiner, P., & Kollman, P. A. (1991) *AMBER 4.0*, University of California, San Francisco.
Riendeau, D., Guay, J., Weech, P. K., Laliberté, F., Yergey, J., Li, C., Desmarais, S., Perrier, J., Liu, S., Nicoll-Griffith, D., & Street, I. P. (1994) *J. Biol. Chem. 269*, 15619.
Roberts, J. D., Yu, C., Flanagan, C., & Birdseye, T. R. (1982) *J. Am. Chem. Soc. 104*, 3945.
Rogers, G. A., & Bruice, T. C. (1974) *J. Am. Chem. Soc. 96*, 2473.
Roshak, A., Sathe, G., & Marshall, L. A. (1994) *J. Biol. Chem. 269*, 25999.
Ryckaert, J. P., Ciccotti, G., & Berendsen, H. J. C. (1977) *J. Comput. Phys. 23*, 327.
Sambrook, J., Fritsch, E. F., & Maniatis, T. (1989) *Molecular Cloning: A Laboratory Manual*, Cold Spring Harbor Press, Cold Spring Harbor, NY.
Scott, D. L., & Sigler, P. B. (1994a) *Adv. Inorg. Biochem. 10*, 139.
Scott, D. L., & Sigler, P. B. (1994b) *Adv. Protein Chem. 45*, 53.
Scott, D. L., Otwinowski, Z., Gelb, M. H., & Sigler, P. B. (1990a) *Science 250*, 1563.
Scott, D. L., White, S. P., Otwinowski, Z., Yuan, W., Gelb, M. H., & Sigler, P. B. (1990b) *Science 250*, 1541.
Scrutton, M. C., & Utter, M. F. (1965) *J. Biol. Chem. 240*, 3714.
Sobotka, A. K., Franklin, R., Adkinson, J., N. F., Valentine, M. D., & Lichtenstein, L. M. (1976) *J. Allergy Clin. Immunol. 57*, 29.

Sprang, S., Standing, T., Fletterick, R. J., Stroud, R. M., Finer-Moore, J., Xuong, N.-H., Hamlin, R., Rutter, W. J., & Craik, C. S. (1987) *Science 237*, 905.

Straatsma, T. P., & McCammon, J. A. (1992) *Annu. Rev. Phys. Chem. 43*, 407.

Tanokura, M. (1983) *Biochim. Biophys. Acta 742*, 576.

Thunnissen, M. M. G. M., Ab, E., Kalk, K. H., Drenth, J., Dijkstra, B. W., Kuipers, O. P., Dijkman, R., De Haas, G. H., & Verheij, H. M. (1990) *Nature 347*, 689.

Verheij, H. M., Volwerk, J. J., Jansen, E. H. J. M., Puyk, W. C., Dijkstra, B. W., Drenth, J., & de Haas, G. H. (1980) *Biochemistry 19*, 743.

Weiner, S. J., Kollman, P. A., Nguyen, D. T., & Case, D. A. (1986) *J. Comput. Chem. 7*, 230.

Zimmerman, S. C., & Cramer, K. D. (1988) *J. Am. Chem. Soc. 110*, 5606.

BI9528412